



POLITECNICO
MILANO 1863

RE.PUBLIC@POLIMI

Research Publications at Politecnico di Milano

Post-Print

This is the accepted version of:

D. Vimercati, A. Guardone

On the Numerical Simulation of Non-Classical Quasi-1d Steady Nozzle Flows: Capturing Sonic Shocks

Applied Mathematics and Computation, Vol. 319, 2018, p. 617-632

doi:10.1016/j.amc.2017.07.033

The final publication is available at <https://doi.org/10.1016/j.amc.2017.07.033>

Access to the published version may require subscription.

When citing this work, cite the original published paper.

© 2018. This manuscript version is made available under the CC-BY-NC-ND 4.0 license
<http://creativecommons.org/licenses/by-nc-nd/4.0/>

Permanent link to this version

<http://hdl.handle.net/11311/1031813>

On the numerical simulation of non-classical quasi-1D steady nozzle flows: capturing sonic shocks

Davide Vimercati^{a,*}, Alberto Guardone^a

^a*Department of Aerospace Science and Technology, Politecnico di Milano
Via La Masa 34, 20156 Milano, Italy*

Abstract

The suitability of Roe-type upwind schemes for the computation of steady quasi-1D flows of non-ideal fluids using explicit integration in the pseudo time is discussed. Based on the particular Roe linearization and entropy fix technique applied, several numerical difficulties can arise in modeling shock waves that are sonic either on the upstream or downstream side of the shock. These so-called sonic shocks typically occur away from stationary points of the cross-sectional area distribution, namely, where the geometrical source term does not vanish. The problem of selecting suitable formulations for the accurate simulation of non-classical quasi-1D steady flows is therefore addressed. Numerical experiments indicate a limited influence of the chosen Roe linearization technique, provided the so-called Property U, allowing the exact representation of steady shocks, is satisfied. Nevertheless, application of standard entropy fixes may either predict an incorrect steady-state transonic expansion neighbouring the sonic shock or even fail to attain a discrete steady state. In the latter case, lack of convergence is due to numerical unbalancing of the flux difference and source term integral over the transonic expansion that occur in the close proximity of sonic shocks approaching their steady-state position. A simple modification to the synchronous splitting technique of van Leer et al. (1989) is proposed, which is able to produce the desired steady-state balance and allows substantial improvement in the resolution of sonic shocks.

Keywords: non-classical gasdynamics, steady-state flows, Roe scheme, source terms

1. Introduction

A dramatic revolution in the theory of compressible fluid dynamics occurs if the so-called fundamental derivative of gasdynamics Γ (Thompson, 1971) defined by

$$\Gamma \equiv 1 + \frac{\rho}{c} \left(\frac{\partial c}{\partial \rho} \right)_s , \quad (1)$$

with ρ , s and c denoting the density, entropy and speed of sound, respectively, becomes negative. The fundamental derivative plays a key role in delineating the dynamic behaviour of compressible-fluid flows (see the early work of Bethe 1942, Zel'dovich 1946, Weyl 1949, Hayes 1958, Thompson 1971), being related, among the others, to the evolution of one-dimensional pressure disturbances and consequent shock formation or fan spreading. The negative sign of Γ implies that the flow field exhibits negative nonlinearity, as opposed to the classical positive nonlinearity characterizing the fluid behaviour in the ideal, perfect-gas limit where $\Gamma > 1$. Together, the regimes of negative ($\Gamma < 0$) and mixed ($\Gamma \gtrless 0$) nonlinearity denote the so-called non-classical gasdynamics. If the flow field occurs entirely in the region $\Gamma < 0$, the fluid dynamics is reversed with respect to the classical case, meaning that, among other things, shock discontinuities carry expansions,

*Corresponding author

Email addresses: davide.vimercati@polimi.it (Davide Vimercati), alberto.guardone@polimi.it (Alberto Guardone)

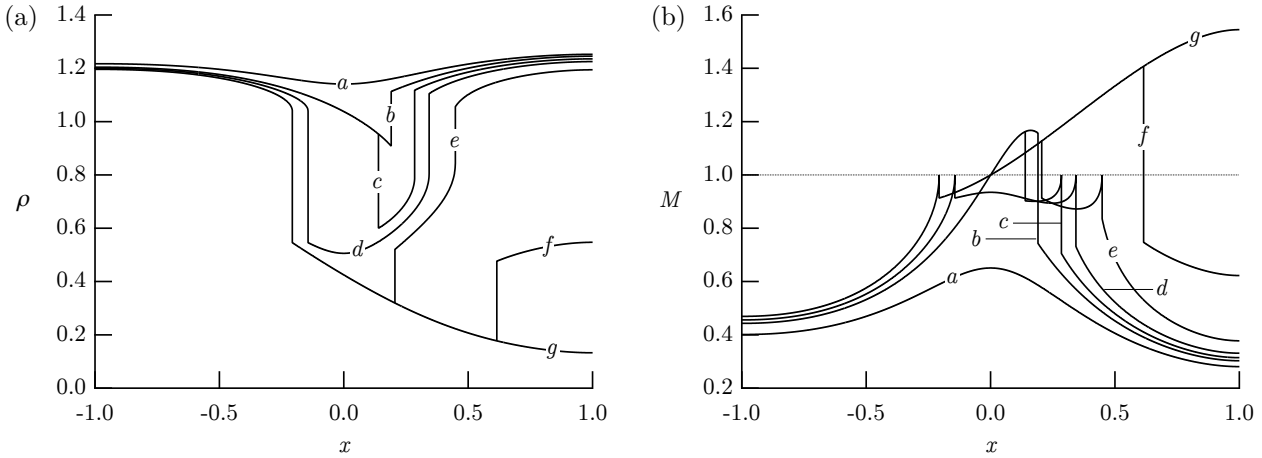


Figure 1: Density (a) and Mach number (b) distributions for selected non-classical flows in a converging-diverging nozzle (the same geometry used in §4), computed from the polytropic van der Waals model with $c_v/R = 50$. The total conditions at the inlet section are fixed; each flow corresponds to a different value of the exhaust pressure.

rather than compressions (see also Thompson and Lambrakis 1973, Cramer and Kluwick 1984, Cramer and Sen 1986). In terms of wave-pattern complexity, however, the regime of mixed nonlinearity is by far the richest, allowing for e.g. sonic shocks and composite waves, see Menikoff and Plohr 1989. This kind of waves can also occur if the fluid undergoes a phase transition because of the loss of convexity at the saturation boundary, though our primary concern here will be non-classical phenomena in single-phase flows. Modern thermodynamic models indicate that peculiar molecularly complex fluids, known as BZT fluids (after Bethe, Zel'dovich and Thompson), embed a finite negative- Γ region in the vapour phase close to the liquid-vapour saturation curve. The interest towards these fluids has grown in the recent past, owing to the fact that non-classical effects could potentially drive towards better efficiencies in applications involving turbomachines and nozzles (see Brown and Argrow, 2000; Zamfirescu and Dincer, 2009; Colonna et al., 2015).

Many practical problems involving compressible-fluid flows can be modelled by considering the quasi-1D Euler system; a typical example being the steady flow of gases through a variable area duct, e.g., a converging-diverging nozzle. Nozzle flows of fluids experiencing mixed nonlinearity can exhibit several and more complex layouts with respect to their ideal-gas counterparts (see Chandrasekar and Prasad, 1991; Kluwick, 1993; Cramer and Fry, 1993; Guardone and Vimercati, 2016). In this respect, Figure 1 reports a set of exact solutions for the density and the Mach number $M = u/c$, where u is the fluid velocity, obtained from the van der Waals model of a BZT fluid expanding across a converging-diverging nozzle. Most of the flow configurations outlined in Figure 1 are peculiar examples of non-classical dynamics; flows having an ideal-gas counterpart are only those of type *a* and *b*, which correspond to a completely subsonic flow and to a choked flow with a compression shock in the diverging section, respectively. Each of the remaining flow fields all include non-classical shock waves. Curve *c* includes a rarefaction shock wave followed by a compression shock with sonic upstream state (also referred to as a pre-sonic compression shock), both in the diverging section of the nozzle. The former shock moves in the converging section, becoming sonic on the upstream side, as the exhaust boundary condition corresponds to the range of type-*d* flows. Any of the subsequent flows *e*-*g* contains a pre-sonic rarefaction shock in the converging section and different configurations downstream of the sonic throat: curve *e* features a so-called split-shock configuration, in which the compression takes place across two different shocks; curve *f* exhibits a single compression shock; curve *g* smoothly expands to supersonic exit Mach numbers. Exact solutions of non-classical steady nozzle flows are discussed in detail by Guardone and Vimercati (2016).

Often, the numerical simulation of conservation laws with source terms, such as the quasi-1D Euler system, is carried out using fractional step methods, in which one alternates the solution of the associated homogeneous system of conservation laws and the solution of a system of ordinary differential equations

in which the source term is the vector field. It is known, however, that fractional step methods can easily fail if the solution is close to a steady state, where the source term must exactly balance the flux gradient (LeVeque, 1998). In order to overcome these difficulties, several unsplit procedures have been proposed (see, e.g., Roe, 1987; Bermudez and Vazquez, 1994; LeVeque, 1998; Bale et al., 2003; Caselles et al., 2009), which mainly rely on upwinding techniques for both the flux gradient and the source term. In this work, we are particularly concerned with numerical schemes that combine an approximate Riemann solver of the Roe type, whose capability of simulating accurately nozzle flows is well assessed (Glaister, 1988; Liou et al., 1990; Mottura et al., 1997; Guardone and Vigevano, 2002; Cinnella, 2006), with an upwind treatment of the source term. The present study is aimed at analysing the behaviour of these schemes in the framework of nozzle flows of non-ideal fluids, which possibly include non-classical waves and multiple sonic points. In this respect, one of the main advantages of a Roe solver is the capability, rooted in the so-called Property U, of capturing steady shocks exactly, which makes this class of schemes particularly suitable for steady-state computations. The latter claim will be confirmed by numerical experiments with an approximate Roe solver (so called because Property U is not satisfied) adopting a simplified procedure for minimal implementation complexity and computational costs.

Since Roe schemes are approximate Riemann solvers, they all must be complemented with a suitable entropy fix in order to prevent the occurrence of entropy violating solutions whenever the flux computed from the approximate solver differs from the exact one. If the steady state includes shocks that are sonic either on the upstream or downstream side, there is possible that a transonic expansion lies in the vicinity of these shocks during convergence to their final, steady-state position. The interaction between the entropy fix and the underlying source term is well-known to be crucial for the steady-state balancing. In this respect, standard corrections (e.g., the entropy fix of Harten and Hyman, 1983) modify the characteristic speed only in the attempt to generate sufficient numerical viscosity; a similar treatment, however, can easily lead to inaccuracies and balancing issues, as the source term is not handled accordingly. The prototypical synchronous entropy fix of van Leer et al. (1989), which operates simultaneously on the characteristic speed and on the source term, is considered. This transonic correction was devised in order to break down sonic glitches in the throat of choked nozzle flows, which are possibly generated by standard entropy corrections. Our numerical experiments will show that the synchronous splitting can efficiently enforce the numerical balance near sonic shocks and that the neighbouring transonic expansion can be cancelled provided the numerical dissipation is adjusted.

This paper is organized as follows. In §2, the governing equations of quasi-1D flows are presented. The computational method is outlined in §3, for which numerical results are presented and discussed in §4. Section 5 presents final remarks and comments.

2. Governing equations

In the present study, the quasi-1D approximation is used to model the steady inviscid flow of a mono-component single-phase fluid through a converging-diverging nozzle. The quasi-1D approximation produces accurate results provided that the radius of curvature of the nozzle axis (the radius or the semi-height for an axisymmetric or 2D nozzle, respectively) is large compared to the nozzle cross-sectional length and that the cross-sectional area $A(x)$ is a smooth function of the axial coordinate x with small variations ($A'(x)/\sqrt{A(x)} \ll 1$), see, e.g., Thompson (1988). The governing equations for smooth flows, namely the quasi-1D Euler equations, can be written in the general form of a balance law for the vector unknown $\mathbf{u} = \mathbf{u}(x, t) \in \Omega \subset \mathbb{R}^p$, $x \in \mathbb{R}$, $t \in \mathbb{R}^+$ as

$$\frac{\partial \mathbf{u}}{\partial t} + \frac{\partial \mathbf{f}(\mathbf{u})}{\partial x} = \boldsymbol{\psi}(\mathbf{u}, x), \quad (2)$$

where

$$\mathbf{u} = (\rho, m, E^t)^T$$

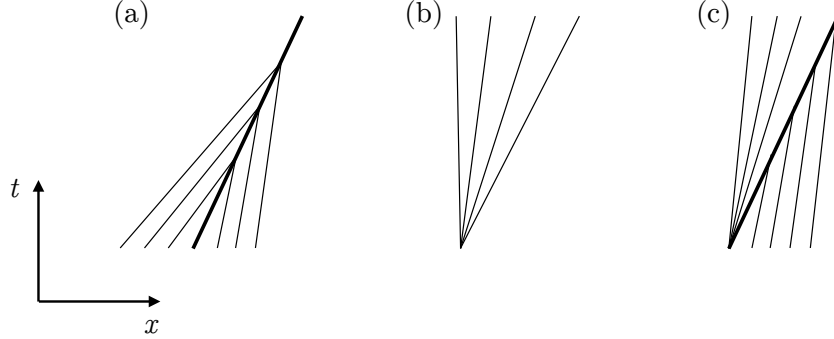


Figure 2: Space-time diagram illustrating exemplary configurations of characteristic lines (thin lines) for (a) genuine shock (thick line), (b) wave fan and (c) simple composite wave consisting of a wave fan terminating into a left-contact shock (thick line).

is the vector of balance variables density ρ , momentum density m and total energy density E^t (internal and kinetic), respectively; $\mathbf{f}(\mathbf{u}) : \Omega \rightarrow \mathbb{R}^p$,

$$\mathbf{f}(\mathbf{u}) = \left(m, \frac{m^2}{\rho} + P(\mathbf{u}), \frac{m}{\rho}(E^t + P(\mathbf{u})) \right)^T$$

is the flux function, where the pressure $P(\mathbf{u})$ is a function of the balance variables and it is computed, for instance, from the equation of state $P(E, \rho)$ for the internal energy density, defined as $E = E^t - m^2/(2\rho)$, and the density. Finally, $\psi(\mathbf{u}, x) : \Omega \times \mathbb{R} \rightarrow \mathbb{R}^p$,

$$\psi(\mathbf{u}, x) = -\frac{A'(x)}{A(x)} \left(m, \frac{m^2}{\rho}, \frac{m}{\rho}(E^t + P(\mathbf{u})) \right)^T$$

is the geometrical source term, where $A(x)$ is the known cross-sectional area distribution along the axial coordinate x . In order to account for discontinuous solutions, system (2) is replaced at the discontinuity location by the well-known Rankine-Hugoniot relation

$$[\mathbf{f}(\mathbf{u})] = s[\mathbf{u}], \quad (3)$$

where $[\cdot]$ indicates the jump between the post-shock and pre-shock states and s is speed of propagation of the discontinuity. Relations (3) must be complemented by suitable admissibility criteria that rule out unphysical shock waves. A sufficient set of conditions is described in detail by, e.g., Kluwick (2004).

The flux Jacobian $\mathbf{A}(\mathbf{u}) \equiv [\partial f_i(\mathbf{u}) / \partial u_j]_{1 \leq i, j \leq p}$ takes the form

$$\mathbf{A}(\mathbf{u}) = \begin{bmatrix} 0 & 1 & 0 \\ -\frac{m^2}{\rho^2} + \frac{\partial P(\mathbf{u})}{\partial \rho} & \frac{2m}{\rho} + \frac{\partial P(\mathbf{u})}{\partial m} & \frac{\partial P(\mathbf{u})}{\partial E^t} \\ \frac{m}{\rho} \left(-\frac{E^t + P(\mathbf{u})}{\rho} + \frac{\partial P(\mathbf{u})}{\partial \rho} \right) & \frac{E^t + P(\mathbf{u})}{\rho} + \frac{m}{\rho} \frac{\partial P(\mathbf{u})}{\partial m} & \frac{m}{\rho} \left(1 + \frac{\partial P(\mathbf{u})}{\partial E^t} \right) \end{bmatrix} \quad (4)$$

and it has real eigenvalues

$$\lambda_1(\mathbf{u}) = \frac{m}{\rho} - c(\mathbf{u}), \quad \lambda_2(\mathbf{u}) = \frac{m}{\rho}, \quad \lambda_3(\mathbf{u}) = \frac{m}{\rho} + c(\mathbf{u}), \quad (5)$$

where the speed of sound $c(\mathbf{u})$ is expressed as a function of the balance variables. In single-phase thermodynamic regions, the speed of sound is strictly positive, so that (2) constitutes a strictly hyperbolic system

of balance laws. The nature of the k -th characteristic field is determined by the so-called nonlinearity factor (see Godlewski), which is defined as

$$\alpha_k(\mathbf{u}) = \nabla_{\mathbf{u}} \lambda_k(\mathbf{u}) \cdot \mathbf{r}_k(\mathbf{u}), \quad (6)$$

where $\nabla_{\mathbf{u}} \lambda_k(\mathbf{u}) \equiv (\partial \lambda_k(\mathbf{u}) / \partial u_i)_{1 \leq i \leq p}$ and $\mathbf{r}_k(\mathbf{u})$ denotes the k -th right eigenvector of the flux Jacobian. The nonlinearity factors for the Euler equations in one space dimension are

$$\alpha_2(\mathbf{u}) = 0, \quad \alpha_{1,3}(\mathbf{u}) = \mp \Gamma(\mathbf{u}), \quad (7)$$

where $\Gamma(\mathbf{u})$ is the fundamental derivative of gasdynamics as a function of the balance variables. While the second characteristic field is always linearly degenerate, the first and third fields could exhibit either genuine nonlinearity, if the flow fully evolves in the regime $\Gamma > 0$ or $\Gamma < 0$, or mixed nonlinearity, if fluid states features both $\Gamma > 0$ and $\Gamma \leq 0$ ¹. Thermodynamics places no constraints on the sign of Γ . In the limit of low pressure and density in which a substance behaves as a perfect gas (i.e., an ideal gas with constant specific heats), the fundamental derivative is a positive constant, namely $\Gamma = (\gamma + 1)/2$, where $\gamma > 1$ is the ratio of the specific heats. In this case, the first and third characteristic fields are genuinely nonlinear and generate genuine (i.e., with characteristic lines impinging on it) compression shocks and rarefaction wave fans. Figure 2 shows exemplary genuine shocks (case a) and wave fans (case b) in the space-time diagram. As it was mentioned in §1, fluids made of complex molecules can exhibit $\Gamma < 0$ in a finite vapour-phase thermodynamic region in the close proximity of the liquid-vapour saturation curve. The gasdynamic restricted to the negative- Γ region is still genuinely nonlinear, but it is reversed with respect to the classical one: shocks carry a rarefaction and wave fans are of the compressive type. A flow field in which the fundamental derivative changes its sign, implying that genuine nonlinearity is lost, can possibly include composite waves, in which several elementary (shocks and fans) waves propagate as a single entity. The simplest of these configurations is represented graphically in the space-time diagram (c) in Figure 2, which consists of a wave fan terminating with a shock wave. Note that for the shock to be contiguous to the fan, it must propagate at the same speed as the edge of the fan. This requires that the shock wave moves at the speed of sound relative to the fluid on one side; such a shock is referred to as a sonic shock or as a one-sided contact shock.

The dependence of systems (2)-(3) from the material properties is embedded in the pressure function in terms of the balance variables. Thus, in order to complete the problem, a suitable thermodynamic model of the fluid must be specified. The simplest model accounting for non-ideal effects is the model of van der Waals (1873) with constant isochoric specific heat (also referred to as polytropic van der Waals model), namely

$$P(T, v) = \frac{RT}{v - b} - \frac{a}{v^2}, \quad c_v = \text{const},$$

where $v = 1/\rho$ is the specific volume, T is the temperature, R is the gas constant and the constants a and b account for the excluded volume and for the intermolecular forces. This model is particularly convenient for qualitative investigations of negative and mixed nonlinearities (see, e.g., Cramer and Sen, 1986; Cramer, 1991; Argrow, 1996; Müller and Voß, 2006). In this respect, the condition $c_v/R \gtrsim 16.67$ must be fulfilled in order that a thermodynamic region featuring $\Gamma < 0$ exists in the vapour phase, see Thompson and Lambrakis 1973. The following numerical investigation will be carried out using the polytropic van der Waals model of a BZT fluid having $c_v/R = 50$.

3. Upwind-differencing schemes for non-homogeneous hyperbolic systems

Let us define a uniform grid $x_j = x_0 + j\Delta x$, $j = 1, \dots, N$, with cell interfaces $x_{j \pm 1/2} = x_j \pm \Delta x/2$, and let $\mathbf{U}_j(t)$ denote the numerical approximation to the cell average of \mathbf{u} over the j th cell, $x \in [x_{j-1/2}, x_{j+1/2}]$.

¹Non-classical shock waves may feature $\Gamma > 0$ both at the pre-shock and at the post-shock state, see Zamfirescu et al. 2008. This, however, requires that the corresponding shock adiabat bridges the thermodynamic region $\Gamma < 0$.

We assume that the approximate solution of (2)-(3) is sought within the computational domain $x \in [x_0, x_N]$ by solving a sequence of interface Riemann problems (Toro, 2013), with initial data given by the piecewise constant states \mathbf{U}_j , of the form

$$\partial_t \mathbf{u} + \hat{\mathbf{A}}_{j+1/2} \partial_x \mathbf{u} = \Delta x \Psi_{j+1/2} \delta(x - x_{j+1/2}), \quad (8)$$

where $\hat{\mathbf{A}}_{j+1/2}$ is an approximate Jacobian and the source term has been replaced by a delta of amplitude $\Psi_{j+1/2}$ located at the cell interface. This treatment of the source term, introduced by Bale et al. (2003) in the context of wave-propagation methods for balance laws, leads naturally to the following wave decomposition,

$$\hat{\mathbf{A}}_{j+1/2}(\mathbf{U}_{j+1} - \mathbf{U}_j) - \Delta x \Psi_{j+1/2} = \sum_p \beta_{j+1/2}^p \mathbf{r}_{j+1/2}^p, \quad (9)$$

where $\mathbf{r}_{j+1/2}^p$ is the p th right eigenvector of the approximate Jacobian. The associated waves of intensity $\beta_{j+1/2}^p$ are thus distributed to the neighbouring cells based on the sign of the corresponding eigenvalues. This procedure yields a semi-discrete scheme of the form

$$\mathbf{U}'_j = -\frac{1}{\Delta x} (\mathbf{F}_{j+1/2} - \mathbf{F}_{j-1/2}) + \frac{1}{2} (\Psi_{j+1/2} + \Psi_{j-1/2}), \quad (10)$$

where the numerical flux $\mathbf{F}_{j+1/2}$ is given by

$$\mathbf{F}_{j+1/2} = \frac{1}{2} (\mathbf{f}(\mathbf{U}_j) + \mathbf{f}(\mathbf{U}_{j+1})) - \frac{1}{2} \sum_p \text{sgn}(\lambda_{j+1/2}^p) \beta_{j+1/2}^p \mathbf{r}_{j+1/2}^p, \quad (11)$$

showing the upwind character of both the flux difference and the source term integral. In the following sections are described the building blocks of our class of schemes, namely the choice of the approximate Jacobian and the discretization of the source term along with the related entropy conditions.

3.1. Roe's linearization for non-ideal gases

One of the most popular and effective approximate Riemann solvers, based on a local linearization of the original nonlinear system, is due to Roe (1981). The basic theory behind the Riemann solver of Roe is here recalled; for a detailed review see, e.g., (LeVeque, 1992). Let \mathbf{u}_l and \mathbf{u}_r denote the left and right states, respectively, in the Riemann problem for the hyperbolic system with flux function $\mathbf{f}(\mathbf{u})$ and flux Jacobian $\mathbf{A}(\mathbf{u})$. A Roe linearization matrix is a constant-coefficient matrix $\hat{\mathbf{A}}(\mathbf{u}_l, \mathbf{u}_r)$ satisfying the following properties, collectively referred to as Property U:

- (i) $\hat{\mathbf{A}}(\mathbf{u}_l, \mathbf{u}_r)(\mathbf{u}_r - \mathbf{u}_l) = \mathbf{f}(\mathbf{u}_r) - \mathbf{f}(\mathbf{u}_l)$.
- (ii) $\hat{\mathbf{A}}(\mathbf{u}_l, \mathbf{u}_r)$ is diagonalizable with real eigenvalues.
- (iii) $\hat{\mathbf{A}}(\mathbf{u}_l, \mathbf{u}_r) \rightarrow \mathbf{A}(\mathbf{u})$ smoothly as $\mathbf{u}_l, \mathbf{u}_r \rightarrow \mathbf{u}$.

The above conditions ensure, in the order specified, the conservation of resulting algorithm, the hyperbolicity of the linearized system and the consistency of the approximation. In addition, in the special case where \mathbf{u}_l and \mathbf{u}_r are connected by a single discontinuity, conditions (i) and (ii) guarantee that the approximate Riemann solution agrees with the exact Riemann solutions.

Once the Roe linearization matrix has been defined, the approximate Jacobian at $x_{j+1/2}$ is obtained by setting $\hat{\mathbf{A}}_{j+1/2} = \hat{\mathbf{A}}(\mathbf{U}_j, \mathbf{U}_{j+1})$. Despite the explicit form of $\hat{\mathbf{A}}(\mathbf{u}_l, \mathbf{u}_r)$ depends on the particular linearization procedure employed, it has been noticed (see Mottura et al., 1997; Guardone and Vigevano, 2002) that two general classes of linearization techniques can be delineated. The first one includes Roe matrices, termed in *Jacobian form*, that are obtained by evaluating the flux Jacobian at a suitable intermediate state $\tilde{\mathbf{u}}(\mathbf{u}_l, \mathbf{u}_r)$, namely

$$\hat{\mathbf{A}}(\mathbf{u}_l, \mathbf{u}_r) = \mathbf{A}(\tilde{\mathbf{u}}(\mathbf{u}_l, \mathbf{u}_r)). \quad (12)$$

With such an approach, condition (ii) is automatically satisfied and (iii) reduces to $\tilde{\mathbf{u}}(\mathbf{u}_l, \mathbf{u}_r) \rightarrow \mathbf{u}$ as $\mathbf{u}_l, \mathbf{u}_r \rightarrow \mathbf{u}$. The intermediate state is obtained from condition (i), which is easily seen to yield a one-parameter family of solutions and thus requires that an additional constraint is specified. For a perfect gas, the additional constraint is an identity, if the velocity $u = m/\rho$ and the total enthalpy per unit mass $h^t = (E^t + P)/\rho$ are chosen as the independent variables. In this case, the renowned Roe averages

$$\tilde{u} = \frac{\sqrt{\rho_l} u_l + \sqrt{\rho_r} u_r}{\sqrt{\rho_l} + \sqrt{\rho_r}} \quad \text{and} \quad \tilde{h}^t = \frac{\sqrt{\rho_l} h_l^t + \sqrt{\rho_r} h_r^t}{\sqrt{\rho_l} + \sqrt{\rho_r}},$$

are recovered. Roe linearizations in Jacobian form are rather uncommon for non-ideal fluids, because of the complexity of the system of equations stemming from condition (i). A notable example is the Roe linearization proposed by Guardone and Vigevano (2002), in which the supplementary condition is selected in order to reduce significantly the complexity associated with the definition of the intermediate state.

An alternative approach stems from the observation that, for a general non-ideal equation of state, only the elements of the *extended* state

$$\mathbf{q} = \left(u, h^t, \frac{\partial P(\mathbf{u})}{\partial \rho}, \frac{\partial P(\mathbf{u})}{\partial m}, \frac{\partial P(\mathbf{u})}{\partial E^t} \right) \quad (13)$$

explicitly occur into the definition (4) of the flux Jacobian (in the perfect-gas case, only u and h^t appear explicitly, owing to the first-degree homogeneity of the corresponding flux function). The so-called linearizations in *quasi-Jacobian form* assume the Roe matrix to be of the form

$$\hat{\mathbf{A}}(\mathbf{u}_l, \mathbf{u}_r) = \mathbf{A}(\tilde{\mathbf{q}}(\mathbf{u}_l, \mathbf{u}_r)), \quad (14)$$

where each of the elements of the intermediate extended state $\tilde{\mathbf{q}}$ is taken as independent unknown of the linearization problem, i.e. the velocity, the total enthalpy and the pressure partial derivative are no longer computed from some state $\tilde{\mathbf{u}}$ (in which case the linearization would indeed be in Jacobian form). The definition of the five parameters is usually carried out by assuming the celebrated Roe averages for the velocity and total enthalpy along with relation

$$\widetilde{\frac{\partial P(\mathbf{u})}{\partial \rho}} = -\tilde{u} \widetilde{\frac{\partial P(\mathbf{u})}{\partial E^t}} \quad (15)$$

to enforce thermodynamic consistency. This procedure reduces the number of degrees of freedom resulting from the imposition of condition (i) to one. Based on the choice of the remaining parameter, many different methods have been derived that include most of the methods available in the scientific literature, such as those due to Abgrall (1991), Cox and Cinnella (1994), Glaister (1988), Grossman and Walters (1989), Liou et al. (1990), Vinokur and Montagné (1990). As pointed out by Toumi (1992), one possible drawback of linearizations in quasi-Jacobian form, with respect to those in Jacobian form, is the lack of a compatible intermediate state, which may lead to inconsistencies whenever the elements of the extended state are used to compute derived thermodynamic quantities. In addition, this approach does not guarantee, in general, that conditions (ii) and (iii) are fulfilled and further constraints could be required.

It has been noticed (see, e.g., Abgrall, 1991; Mottura et al., 1997), however, that none of these formulations was proved to be clearly superior to the others, while, on the other hand, the numerical efficiency is largely influenced by the complexity of a particular formulation. In this respect, most difficulties in the computation of $\hat{\mathbf{A}}$ lie with condition (i) of Property U. This ultimately led some researchers to adopt solvers which do not satisfy exactly condition (i), but only in some approximate manner (thus, they are not formally Roe schemes and will be referred to as approximate Roe solvers), and still give reasonably accurate results, see Masella et al. (1999), Buffard et al. (2000), Cinnella (2006). These simplified procedures sacrifice some of the advantages of an exact (in the sense that Property U is satisfied exactly) linearization in order to minimize implementation complexity and computational costs.

To the authors' knowledge, there does not exist any study of the performance of these Roe-type linearizations when applied to the computation of steady nozzle flows of non-ideal gases, that possibly include

non-classical waves. Thus, our numerical experiments will initially focus on the assessment of selected linearization procedures. Three formulations will be tested as representative of different linearization philosophies: the solvers of Guardone and Vigevano (2002) and of Vinokur and Montagné (1990) as representative of the exact linearizations in Jacobian and quasi-Jacobian form, respectively, and the simplified formulation of Cinnella (2006) as representative of the approximated linearization procedures.

3.2. Source term discretization

The Roe schemes described above require that some sort of discretized form of the source term $\Psi_{j+1/2}$ is defined at cell edges. Note that, if the interface values $\Psi_{j+1/2}$ approximate the source term to $\mathcal{O}(\Delta x^2)$, then the resulting scheme (10)-(11) is second-order accurate in space (it is easy to see that each flux difference and source term integral are centred on the same interval). In this work, we use the simple average

$$\Psi_{j+1/2} = \frac{1}{2}(\psi(\mathbf{U}_j, x_j) + \psi(\mathbf{U}_{j+1}, x_{j+1})) \quad (16)$$

to discretize the source term, even though this choice will not yield a well-balanced scheme, i.e. initial equilibrium values would not be preserved by the method. As discussed by LeVeque (2011), a suitable average resulting in a well-balanced scheme can be conveniently defined for diverse problems; these, unfortunately, do not include the quasi-1D Euler equations. However, in most numerical experiments for which our scheme appropriately models the flow field (recognizing, for instance, transonic expansion or non-classical composite waves), the residual of the solution is as low as 10^{-10} and the scheme is found to be balanced almost to machine precision.

3.3. Sonic entropy correction

The upwind contribution to the interface flux along the p th right eigenvector \mathbf{r}^p in (11) can be written as

$$\operatorname{sgn}(\lambda^p)\beta^p = |\lambda^p|\alpha^p - \operatorname{sgn}(\lambda^p)z^p\Delta x, \quad (17)$$

where we have used $\mathbf{U}_{j+1} - \mathbf{U}_j = \sum_p \alpha^p \mathbf{r}^p$ and $\Psi_{j+1/2} = \sum_p z^p \mathbf{r}^p$ (subscript $j + 1/2$ has been dropped for brevity). If a transonic expansion occurs at the interface Riemann problem, namely if the data are such that $\lambda_j^p < 0 < \lambda_{j+1}^p$, the eigenvalue λ^p of the dissipation matrix can possibly vanish, thus leading to the formation of entropy-violating shocks (with outgoing characteristics). Popular transonic entropy fixes are those due to Harten (1983), Harten and Hyman (1983), LeVeque (1992) or Kermani and Plett (2001), which rely on the model of a smooth transonic expansion wave to generate a sufficient amount of numerical viscosity. These transonic fixes lead to redefine in some way the characteristic speed near a sonic point; for instance, in the case of the Harten and Hyman (1983) correction, $|\lambda^p|$ is replaced by

$$|\lambda^p|^* = \frac{1}{2} \left(\frac{(\lambda^p)^2}{\delta_\lambda^p} + \delta_\lambda^p \right), \quad (18)$$

where $\delta_\lambda^p = \max(0, \lambda^p - \lambda_j^p, \lambda_{j+1}^p - \lambda^p)$ controls the band over which the entropy correction is enforced. The above mentioned entropy corrections have been successfully employed to break down entropy-violating shocks in both unsteady and steady-state problems governed by hyperbolic conservation laws. However, direct application of any of these sonic fixes to systems incorporating source term may lead to unsatisfactory results, especially when a steady-state solution is sought. The most noticeable defect, as shown by van Leer et al. (1989), consists in a two-cell sonic plateau placed at the throat of steady nozzle flows in choked conditions, where the transition from subsonic to supersonic flow takes place. In the work of van Leer et al. (1989) a cure to this problem, known as the entropy bypass, is proposed. The entropy bypass consists in the synchronous splitting of the characteristic speed and of the source term near a sonic point. If a transonic rarefaction is detected, namely if $\lambda_j^p < 0 < \lambda_{j+1}^p$, the average values $\bar{\lambda}^p = (\lambda_j^p + \lambda_{j+1}^p)/2$, $\bar{z}^p = (z_j^p + z_{j+1}^p)/2$ and the spreading $\delta_\lambda^p = d_{\text{ef}}(\lambda_{j+1}^p - \lambda_j^p)$, $\delta_z^p = d_{\text{ef}}(z_{j+1}^p - z_j^p)$ for both the characteristic speed and the source term can be recognized. These are used to compute the effective absolute value $|\lambda^p|^*$,

$$|\lambda^p|^* = \frac{(\bar{\lambda}^p)^2}{\delta_\lambda^p} + \frac{\delta_\lambda^p}{4}, \quad (19)$$

Test Case	Inlet			Outlet		
	P/P_c	ρ/ρ_c	M	P/P_c	ρ/ρ_c	M
TC1	1.3295	1.3056	0.4655	1.3210	1.2955	0.3832
TC2	1.0708	1.1964	0.4695	1.0707	1.1946	0.3778
TC3	0.1658	0.0083	0.6070	0.0468	0.0024	1.7000
TC4	1.0726	1.2000	0.4561	1.0847	1.2253	0.3314
TC5	1.0829	1.2223	0.4415	0.3206	0.1418	1.5178

Table 1: Inlet ($x = -1$) and outlet ($x = 1$) boundary conditions for each of the test cases. P/P_c and ρ/ρ_c denote the reduced pressure and reduced density, respectively, where subscript c indicates critical-point values); M is the flow Mach number.

which is used in place of $|\lambda^p|$ and the effective source term z^{p*} ,

$$z^{p*} = \frac{\bar{\lambda}^p}{\delta_\lambda^p} \left(2\bar{z}^p - \bar{\lambda}^p \frac{\delta_z^p}{\delta_\lambda^p} \right) + \frac{\delta_z^p}{4}, \quad (20)$$

which is used in place of $\text{sgn}(\lambda^p)z^p$ in (17). As pointed out by van Leer et al. (1989), adding a suitable splitting of the source term to that of the characteristic speed, in the presence of transonic expansions, allows to smoothly match the backward and forward facing parts of the fan while the sonic point is approaching its final position in the throat (where the source term vanishes), thus avoiding sonic plateaus in the steady-state solution. The above transonic flux formula contains a free parameter d_{ef} controlling the spreading of the expansion fan. In their numerical experiments, van Leer et al. (1989) report that $d_{\text{ef}} = 2 \div 4$ allows to reach the correct steady-state flow at a sonic throat, starting from arbitrary initial conditions, whereas lower values of d_{ef} would result in the formation of a sonic plateau. The analysis of Goodman and LeVeque (1988) also indicates that optimal robustness in handling a sonic throat is obtained with $d_{\text{ef}} = 4$.

In the following numerical experiments, scheme (10)-(11) for the Jacobian, quasi-Jacobian and simplified formulation of the Roe matrix will at first be tested along with different entropy corrections. To the best of the authors' knowledge, there has been no investigation on the effectiveness of this class of schemes in steady-state computations of non-ideal, possibly non-classical, nozzle flows. Next, the performance of the synchronous splitting of van Leer et al. (1989) will be studied, with particular emphasis on the role of the artificial spreading of the expansion fan.

4. Numerical results

In this section, the upwind schemes described above are applied to the solution of a set of steady nozzle flows of BZT fluids, which are all modelled as van der Waals gases with $c_v/R = 50$. All computations refer to a conventional converging-diverging geometry, whose cross-sectional area distribution is given by

$$A(x) = -0.225x^5 - 0.35x^4 + 0.375x^3 + 0.7x^2 + 1, \quad x \in [-1, 1]. \quad (21)$$

The streamwise locations $x = -1, 0, 1$ denote the inlet, throat and exit sections, respectively. A 400-cell uniform computational grid is used throughout this work. The boundary conditions for the test cases considered in the following are reported in Table 1. Characteristic boundary treatment is used. Solutions are marched in time with the forward Euler time stepping (we are not interested in temporal accuracy). The CFL number is set to 0.8. The initial condition for each of the test cases is a constant distribution of the mass flow rate and a linear distribution of pressure and density matching the boundary conditions. No flux limiter will be used, insofar as scheme (10)-(11), in which any of the above-mentioned Roe solvers is used along with treatment (16) for the source term, will yield second-order accurate steady state solutions. Local time stepping is used to speed up convergence to the steady state. The 2-norm of the time derivative of the numerical solution is used as stopping criteria: when this residual is 10^{-10} times a reference residual (computed in the initial stages of the time marching), the flow is considered steady. The exact solutions,

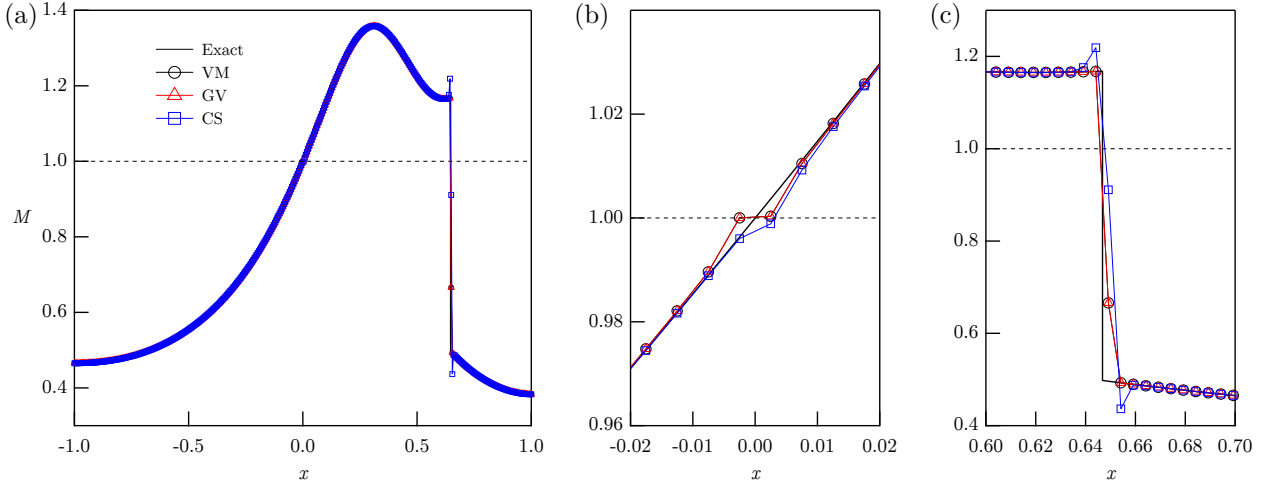


Figure 3: TC1-HH: comparison of the Mach number distributions obtained with the Roe solvers evaluated and the entropy correction of Harten and Hyman on a non-ideal, yet classical, shocked nozzle flow. (a) Complete flow field; (b) enlargement of the throat region; (c) enlargement of the shock wave in the diverging section.

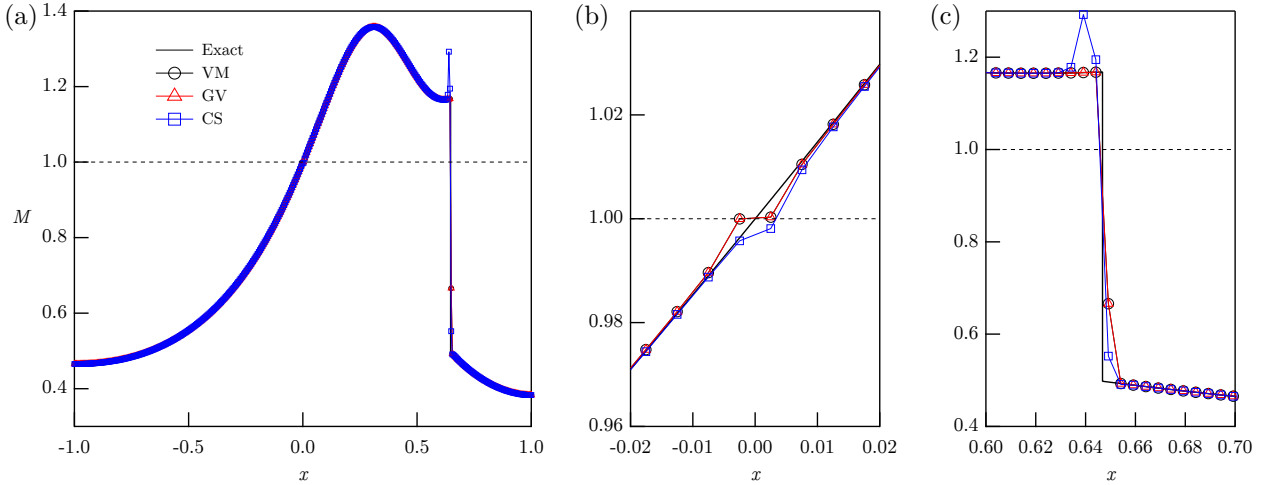


Figure 4: TC1-LV: same as Figure 3 but with LeVeque's entropy correction.

to which our numerical results are compared, are computed using the shock-fitting technique described by Guardone and Vimercati (2016).

4.1. Assessment of selected Roe solvers and entropy fixes

To begin with, the effect of one particular choice of the Roe solver and of the entropy correction is discussed. The Roe formulations examined here are the exact solvers due to Vinokur and Montagné (1990), Guardone and Vigevano (2002) and the approximate solver of Cinnella (2006). The shorthand “VM”, “GV” and “CS”, respectively, will be used for the three solvers to be tested. At sonic points, the entropy corrections of Harten and Hyman (1983), LeVeque (1992) and Kermani and Plett (2001) are considered, to be referred to as “HH”, “LV” and “KP” corrections, respectively.

In our first test case, denoted as TC1, the inlet pressure and density are selected in the dense-gas thermodynamic region at slightly supercritical conditions. The exit boundary data is such that the steady-

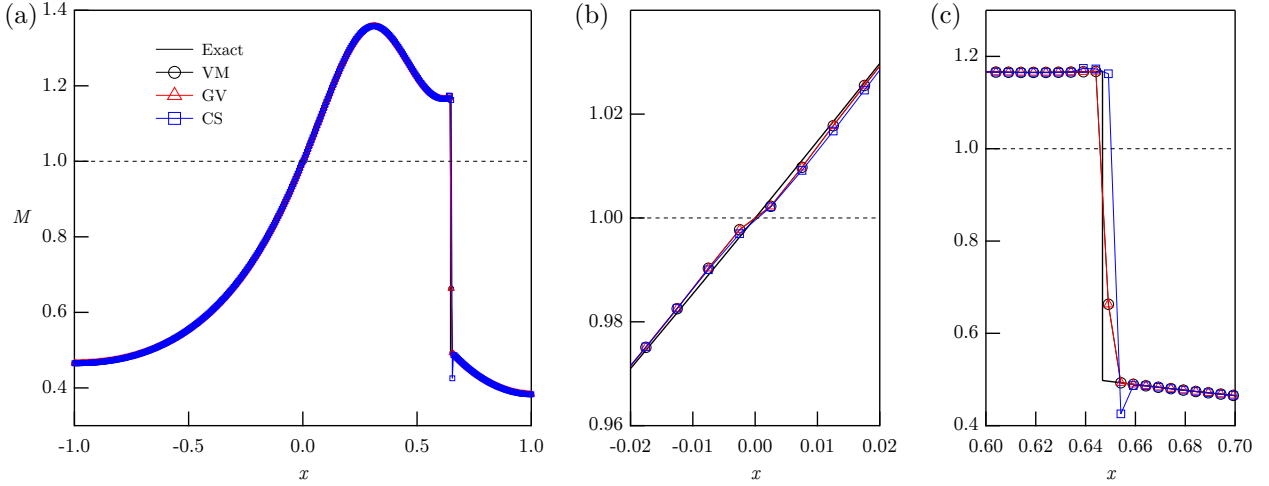


Figure 5: TC1-KP: same as Figure 3 but with Kermani and Plett's entropy correction.

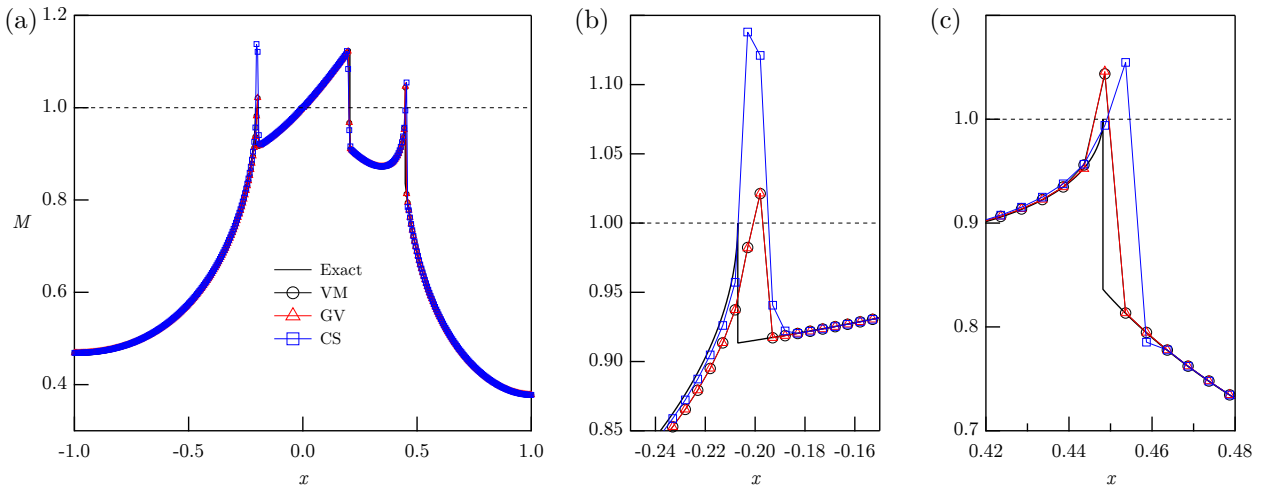


Figure 6: TC2-HH: comparison of the Mach number distributions obtained with the Roe solvers evaluated and the entropy correction of Harten and Hyman on a non-classical nozzle flow with three shock waves, two of which have sonic upstream state. (a) Complete flow field; (b) and (c) enlargements of the sonic shocks

state solution features a subsonic to supersonic transition in the throat and a compression shock wave in the diverging section. The computed Mach number distributions are shown in Figures 3-5 along with the exact solutions; the corresponding convergence histories are reported in Figures 13a-c. Note that the scheme obtained with the CS solver and LV entropy fix failed to converge; the Mach number distribution reported in Figure 4 is a snapshot extracted from the limit cycle in which the computation is trapped. The considered Roe formulations exhibit similar performances in smooth regions of the flow field: the solutions of the VM and GV solvers are always superposed and CS performs only slightly different, owing to the fact that the latter satisfies Property U to within $\mathcal{O}(\|\mathbf{u}_r - \mathbf{u}_l\|^2)$. However, none of the transonic entropy fix examined here is able to produce a perfectly smooth transition in the throat of the nozzle (see enlargements in Figures 3-5). Here, the closest agreement with the exact solutions is obtained with the KP correction, owing to the larger band over which the correction is enforced and the correspondingly larger artificial numerical viscosity introduced (see Kermani and Plett, 2001). The two-cell plateau that is computed when the sonic point is

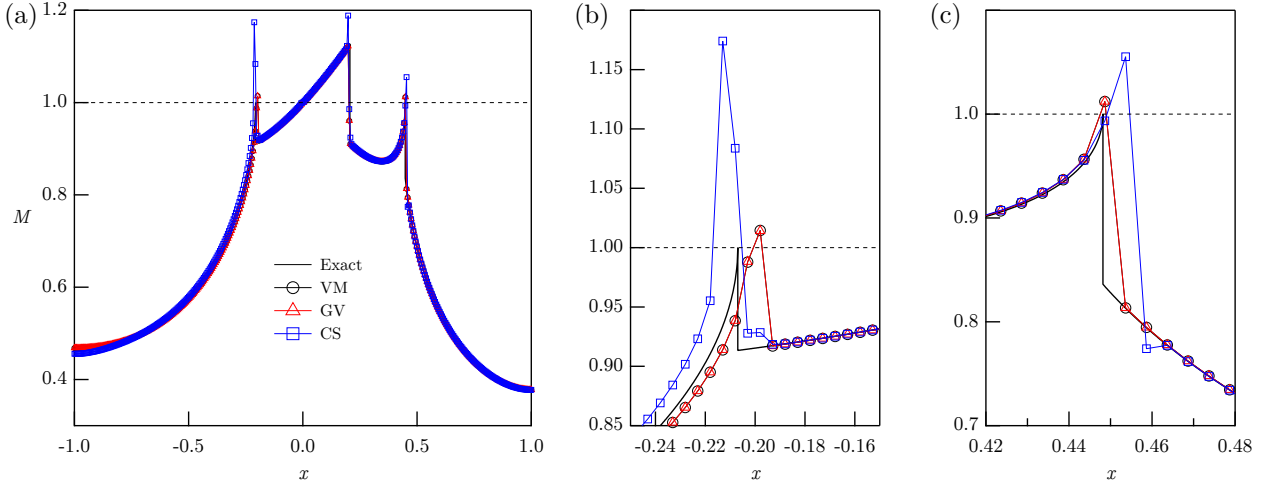


Figure 7: TC2-LV: same as Figure 6 but with LeVeque's entropy correction.

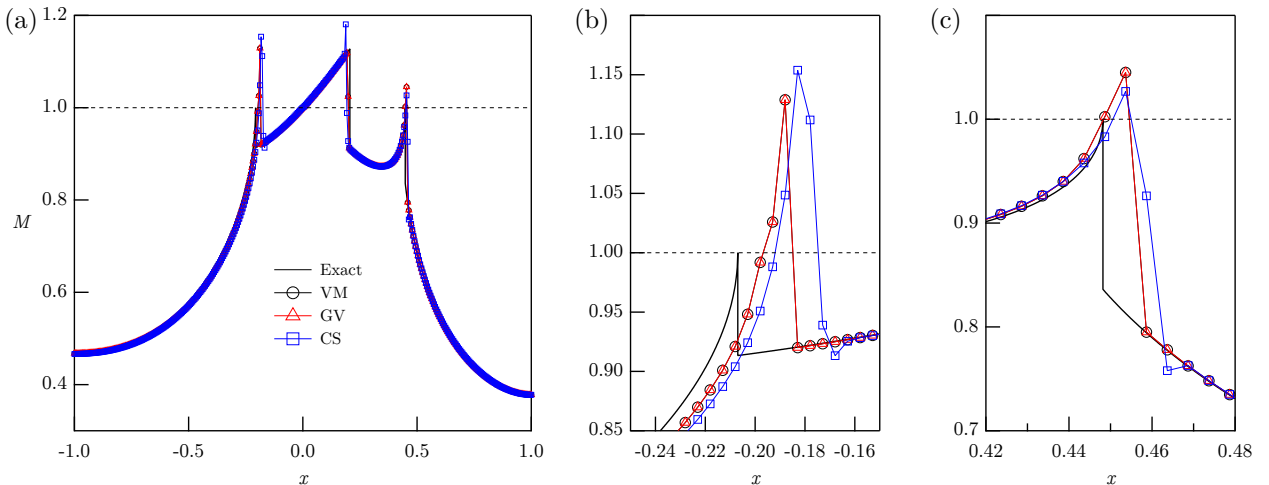


Figure 8: TC2-KP: same as Figure 6 but with Kermani and Plett's entropy correction.

approaching the throat also causes slow convergence towards the steady state. This agrees with the analysis of van Leer et al. (1989). As for the behaviour of the three solvers near discontinuities (see enlargements in Figures 3-5), the exact solvers (VM and GV) are considerably more accurate than the simplified procedure. While the VM and GV formulations produce sharp shock profiles, the CS solver introduces large oscillations both upstream and downstream of the discontinuity. Presumably, this effect is a direct consequence of the larger numerical viscosity introduced by the simplified procedure, which is not capable of capturing steady shocks across a single cell interface and tends to smear the discontinuities across multiple cells.

Next, a more challenging test case is considered. Boundary data for TC2 have been selected to obtain three discontinuities within the nozzle, as shown in Figures 6-8. The first one is a rarefaction shock with sonic upstream state, located upstream of the throat; the second one is a classical compression shock just downstream of the throat; the third one is a compression shock with sonic upstream state. All the simulations carried out with the HH and LV entropy corrections failed to converge, see the convergence histories in Figures 13d-f; the Mach number distribution reported in Figures 6 and 7 are snapshots extracted from the limit cycle in which the computations ended. The analysis of the residual's distribution reveals that, using

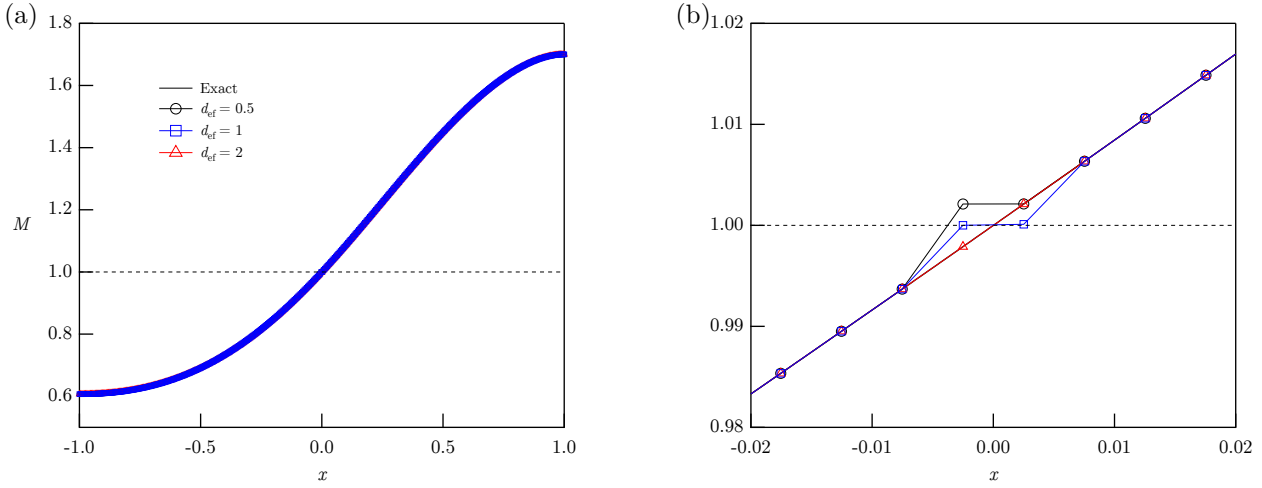


Figure 9: TC3: Mach number distributions obtained from the GV solver with equipped with the entropy bypass on a smooth nozzle flow expanding from subsonic inlet conditions to supersonic exit conditions. (a) Complete flow field; (b) enlargement of the throat section.

HH and LV fixes, balancing issues occur at cell interfaces neighbouring the sonic shocks on the upstream side, where a transonic expansion is computed in time marching from the initial distribution of the balance variables and prevents the solution from reaching a steady state. On the contrary, no balancing issues occur using the KP fix; the larger bandwidth of this correction guarantees a numerical steady state solution. Nevertheless, none of the considered Roe solvers and entropy fixes is accurate in the close proximity of sonic shocks (the KP fix, in this respect, is the most inaccurate), nor in the throat section as already observed in the previous test case.

Similarly to TC1, the exact solvers seem to perform better than the simplified solver. Moreover, if the TC2 simulations are initialised using the exact steady-state solution, which does not include transonic expansions near the sonic shocks, the method equipped with either VM or GV solvers preserves the initial distribution without adding sonic points; on the other hand, the CS solver produces a distribution similar to that reported in Figures 6-8 (without converging to a steady state). The latter observation suggests that, for the exact solvers, the inaccuracies near sonic shocks and the lack of convergence to the steady state can be eliminated or reduced by using more sophisticated entropy corrections accounting for the presence of the background source term. In contrast, the glitches exhibited by the simplified solver should be ascribed not only to the entropy fix, but also to the solver itself, thus pointing again to the benefits (rooted in Property U) of a sharp-shock representation.

4.2. The entropy bypass for capturing sonic shocks

The assessment of the different Roe solvers carried out in the previous section calls attention to the superior performances of the exact solvers for steady-state calculations. In this respect, the GV and VM solvers showed negligible differences in the numerical results. In the following, we will examine the behaviour of an exact Roe solver in conjunction with entropy corrections that are able to produce the desired steady state balance and accuracy near sonic shock wave. Without loss of generality, the GV solver will be considered herein (calculations performed with the VM solver, not shown here, show indeed minimal differences). The next series of numerical experiments will take advantage of the transonic treatment of van Leer et al. (1989), referred to by the authors themselves as the entropy bypass (“EB” in the following). The entropy bypass, see relations (19)-(20), is based on a synchronous splitting of the characteristic speed and source term integral near a sonic point. Such a joint treatment, devised in the context of classical nozzle flows to fix sonic glitches in the throat of choked nozzle flows, can be successfully applied to non-classical flows including sonic shocks, see below.

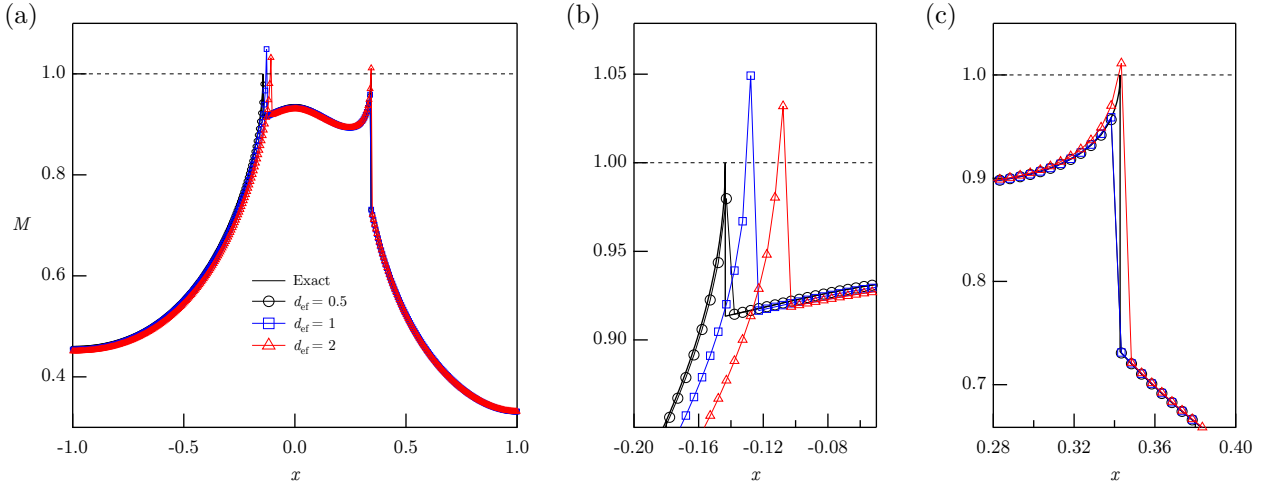


Figure 10: TC4: Mach number distributions obtained from the GV solver with the entropy bypass on a non-classical flow including two sonic shocks (both on the upstream side) but no supersonic points. (a) Complete flow field; (b) and (c) enlargements of the leading and trailing sonic shocks, respectively.

Before commenting on the possibility of obtaining accurate representation of sonic shocks, we consider a smooth choked flow, indicated as TC3 in Table 1, expanding from subsonic inlet conditions to supersonic exit conditions. Thus, at the steady state, a transonic expansion is located in the throat of the nozzle, which is precisely the situation for which the EB transonic formula was originally formulated. The effectiveness of the simultaneous splitting of the characteristic speed and the source term is shown in Figure 9. Our numerical results are consistent with the previous findings: if the spreading parameter is sufficiently large, namely $d_{\text{ef}} = 2$ according to the analysis of van Leer et al. (1989), the sonic plateau is removed. On the contrary, the choices $d_{\text{ef}} = 0.5$ and $d_{\text{ef}} = 1$ lead to the same inaccuracies observed in TC1 (though here the convergence to the steady state was faster, see Figure 13g for the convergence histories).

We turn now to a non-classical nozzle flow which represents, in a sense, the opposite scenario of the previous test case and it is used here to evaluate the behaviour of the synchronous splitting near sonic shocks. The flow field for TC4 includes two shock waves with sonic upstream states, but no supersonic points. Numerical results obtained with different values of the spreading parameter are shown in Figure 10 and the corresponding convergence histories are reported in Figure 13h. The computations performed with $d_{\text{ef}} = 0.5$ and $d_{\text{ef}} = 1$ converged to the steady state, suggesting that the entropy bypass at sonic points can possibly balance transonic expansions even when these are located far from the throat, namely, where the source term does not vanish. Most importantly, the amplitude of the transonic expansion that is incorrectly computed during time marching can be reduced by decreasing the value of the spreading parameter of the model fan. Eventually, using $d_{\text{ef}} = 0.5$ the transonic expansion is completely removed and the errors in the location of the sonic shock is significantly reduced.

The effect of the parameter d_{ef} on the spreading of the transonic fan can be explained as follows. As the sonic shock approaches its steady-state position, the solution of the Riemann problem at the corresponding cell interface will have, in general, the structure of a composite wave as shown, for instance, in Figure 2 for the exemplary case of a left contact shock. In this respect, the larger the spreading of the model expansion fan in the entropy correction formula, the larger will be the smooth fan in the composite wave. Thus, with large values of d_{ef} , the sonic shock will be wrongly captured as a transonic expansion–genuine shock combination.

4.3. An improved formula

The present analysis allows us to clarify two important aspects related to the treatment of sonic points in steady nozzle flows. Firstly, if the source term is not modified jointly with the characteristic speed, large

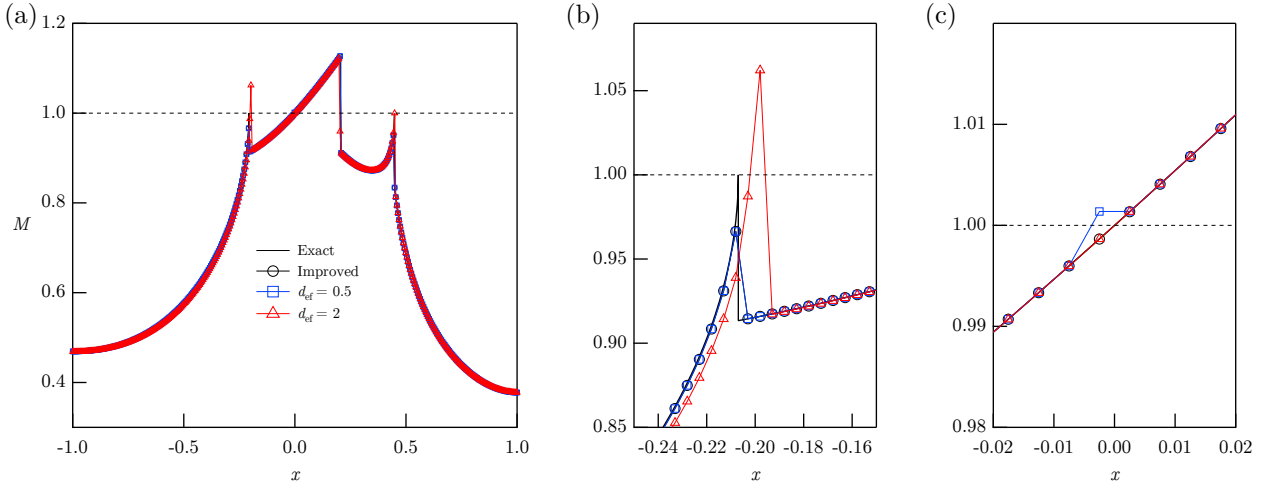


Figure 11: TC2-EB: comparison of the Mach number distributions obtained from the GV solver equipped with the plain and improved entropy bypass. (a) Complete flow field; (b) enlargement of the leading sonic shock; (c) enlargement of the throat region.

inaccuracies can be found either in the throat of choked flows and in proximity of sonic shocks. In the latter condition, one also has to expect unbalancing problems that destroy the convergence towards the steady state, unless a large band entropy fix, such as the KP one, is used. The second relevant consideration is that the synchronous splitting can efficiently break down sonic plateaus and provide steady-state balance even when a transonic rarefaction is computed in the time advance. However, in order to meet these goals and, in particular, to improve resolution of sonic shocks, the spreading of the transonic fan in the entropy correction should be specifically adjusted. On the one hand, large values of d_{ef} guarantee perfectly smooth subsonic to supersonic expansions in the throat of choked flows; on the other hand, lower values of d_{ef} allow to improve the resolution of sonic shocks. The fact that, at the steady state, subsonic to supersonic transition can take place only at the throat, while sonic shocks occur away from it (except for very special boundary data, see Guardone and Vimercati 2016), suggests that a possible way to deal with non-classical steady nozzle flows is to adapt d_{ef} to the the various regions of the nozzle. The simplest approach, in this sense, would consist in selecting a small value of d_{ef} everywhere except in the nozzle throat, where a larger spreading parameter is triggered to provide an appropriate amount of numerical dissipation in case a transonic expansion occurs at the steady state.

This simple treatment of the sonic points is tested again on TC2, see Figure 11. Here we have reported the numerical solutions obtained from the plain EB correction with $d_{ef} = 0.5$ and $d_{ef} = 2$, whose inaccuracies have been previously discussed, and the numerical results of the mixed approach, which is denoted as “improved”. The improved procedure is constructed by imposing $d_{ef} = 0.5$ everywhere except for few interfaces neighbouring the throat, where $d_{ef} = 2$ is triggered. Here, the empirical choice $d_{ef} = 0.5$ for handling sonic shocks away from the throat is motivated by the parametric study shown in Figure 10. On the other hand, the choice of the throat value $d_{ef} = 2$ is consistent with the analysis of (van Leer et al., 1989) and with our numerical experiments shown in Figure 9. The same procedure is applied to TC5, shown in Figure 12, which exhibits a post-sonic shock in the diverging section of the nozzle. In both cases, the improved treatment of transonic expansions makes it possible to combine the advantages of the choice $d_{ef} = 2$ in the sonic throat and the enhanced resolution of sonic shocks provided by $d_{ef} = 0.5$. For both TC2 and TC5, the improved method converges rapidly to the exact steady state, see Figures 13i-j.

Admittedly, the simple modification described above can be unsatisfactory if the exact steady state contains a sonic shock at the throat (this can possibly occur for special boundary data marking the transition between different functioning regimes of the nozzle, see Guardone and Vimercati 2016). A more robust and general entropy correction would consist in adapting the spreading parameter only when a sonic or nearly

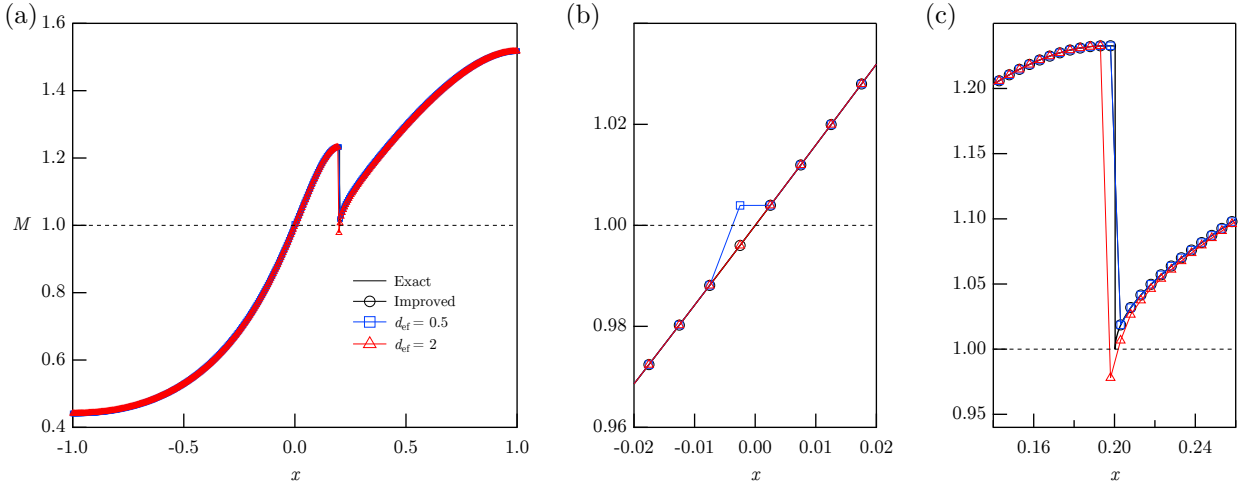


Figure 12: TC5: comparison of the Mach number distributions obtained from the GV solver equipped with the plain and improved entropy bypass. The flow field features a shock with downstream sonic state in the diverging section and a subsonic to supersonic transition in the throat of the nozzle. (a) Complete flow field; (b) enlargement of the throat region; (c) enlargement of the sonic shock.

sonic shock is detected. This would require, in turn, the definition of a general procedure for detecting sonic shock. The design of such an enhanced treatment is left for future investigations.

5. Conclusions

A class of upwind schemes for the computation of quasi-1D steady flows of non-ideal fluids, possibly exhibiting non-classical phenomena such as rarefaction and sonic shocks, was evaluated. The considered schemes combine an approximate Riemann solver of the Roe type with a simple upwind treatment of the source term, yielding a formal second-order discretization on smooth steady-state solutions provided that the source term is computed accordingly (for instance, by simply averaging the values from cells neighbouring the considered interface). Explicit integration with local time stepping in the pseudo time is used to converge to steady state.

The numerical analysis was carried out for converging-diverging nozzle geometries, though it is valid for all quasi-1D geometries. The present study pointed out that care must be exercised in the choice of both the Roe solver and the entropy correction formula. The Roe solvers due to Guardone and Vigevano (2002), Cinnella (2006) and Vinokur and Montagné (1990) were first evaluated as representative of the different families of linearization procedure available in the literature. If coupled with a standard entropy fix operating on the characteristic speed only, such as the popular fixes due to Harten and Hyman (1983), LeVeque (1992) or Kermani and Plett (2001), the evaluated solvers were found to deliver inaccurate results related to the treatment of sonic points, in addition to being slow or unable to converge to the steady state. Two major sources of error were detected: a sonic plateau computed in the throat of choked nozzle flows and a transonic expansions in the vicinity of sonic shocks approaching the steady-state position. In the latter case, the unbalance between the flux and source terms possibly force the shock itself to oscillate in a limit cycle. In this respect, low-dissipation entropy corrections, such as the Harten and Hyman's or LeVeque's fixes, are particularly prone to unbalancing and convergence issues. Moreover, the solver's capability of capturing steady shocks exactly (the so-called Property U) was shown to be essential for the accurate numerical modeling of steady-state shocked nozzle flows, especially for those including sonic shocks.

Following these considerations, the behaviour of the synchronous entropy fix of van Leer et al. (1989), known as the entropy bypass, was examined along with the formulation of Guardone and Vigevano (negligible differences where observed with Vinokur and Montagné's formulation), with the aim of eliminating the

sonic plateau at the nozzle throat (for which this fix was originally designed) and of producing the desired steady-state balance and accuracy near sonic shocks. Our numerical experiments showed that these goals can be accomplished with the proper choice of the free parameter d_{ef} controlling the rate of spreading of the model expansion fan. However, the two purposes were seen to be conflicting, inasmuch as larger values of d_{ef} guarantee smooth transitions in the nozzle throat, whereas lower values allow to reduce and eventually remove the transonic expansion neighbouring sonic shock in the numerical steady state. A simple improvement of the synchronous entropy correction, in which the spreading parameter is locally adapted to the different regions of the nozzle, was proposed and successfully tested. This idea could be further explored to design more sophisticated entropy corrections.

Acknowledgements

This research is supported by ERC Consolidator Grant N. 617603, Project NSHOCK, funded under the FP7-IDEAS-ERC scheme.

References

- Abgrall, R., 1991. An extension of Roe's upwind scheme to algebraic equilibrium real gas models. *Comput. & Fluids* 19 (2), 171–182.
- Argrow, B. M., 1996. Computational analysis of dense gas shock tube flow. *Shock waves* 6 (4), 241–248.
- Bale, D. S., LeVeque, R. J., Mitran, S., Rossmanith, J. A., 2003. A wave propagation method for conservation laws and balance laws with spatially varying flux functions. *SIAM J. Sci. Comput.* 24 (3), 955–978.
- Bermudez, A., Vazquez, M. E., 1994. Upwind methods for hyperbolic conservation laws with source terms. *Comput. & Fluids* 23 (8), 1049–1071.
- Bethe, H. A., 1942. The theory of shock waves for an arbitrary equation of state. Technical paper 545, Office Sci. Res. & Dev.
- Brown, B. P., Argrow, B. M., 2000. Application of Bethe-Zel'dovich-Thompson fluids in Organic Rankine Cycle engines. *J. Propul. Power* 16 (6), 1118–1123.
- Buffard, T., Gallouët, T., Hérard, J. M., 2000. A sequel to a rough Godunov scheme: application to real gases. *Comput. & Fluids* 29 (7), 813–847.
- Caselles, V., Donat, R., Haro, G., 2009. Flux-gradient and source-term balancing for certain high resolution shock-capturing schemes. *Comput. & fluids* 38 (1), 16–36.
- Chandrasekar, D., Prasad, P., 1991. Transonic flow of a fluid with positive and negative nonlinearity through a nozzle. *Phys. Fluids A* 3 (3), 427–438.
- Cinnella, P., 2006. Roe-type schemes for dense gas flow computations. *Comput. & Fluids* 35 (10), 1264–1281.
- Colonna, P., Casati, E., Trapp, C., Mathijssen, T., Larjola, J., Turunen-Saaresti, T., Uusitalo, A., 2015. Organic Rankine Cycle power systems: From the concept to current technology, applications, and an outlook to the future. *J. Eng. Gas Turb. Power* 137 (10), 100801–1–19.
- Cox, C. F., Cinnella, P., 1994. General solution procedure for flows in local chemical equilibrium. *AIAA J.* 32 (3), 519–527.
- Cramer, M. S., 1991. Nonclassical dynamics of classical gases. In: Kluwick, A. (Ed.), *Nonlinear Waves in Real Fluids*. Springer-Verlag, New York, NY, pp. 91–145.
- Cramer, M. S., Fry, N. R., 1993. Nozzle flows of dense gases. *Phys. Fluids A* 5 (5), 1246–1259.
- Cramer, M. S., Kluwick, A., 1984. On the propagation of waves exhibiting both positive and negative nonlinearity. *J. Fluid Mech.* 142, 9–37.
- Cramer, M. S., Sen, R., 1986. Shock formation in fluids having embedded regions of negative nonlinearity. *Phys. Fluids* 29, 2181–2191.
- Glaister, P., 1988. An approximate linearised Riemann solver for the Euler equations for real gases. *J. Comput. Phys.* 74 (2), 382–408.
- Goodman, J. B., LeVeque, R. J., Apr. 1988. A geometric approach to high resolution TVD schemes. *SIAM J. Numer. Anal.* 25 (2), 268–284.
- Grossman, B., Walters, R. W., 1989. Analysis of flux-split algorithms for Euler's equations with real gases. *AIAA J.* 27 (5), 524–531.
- Guardone, A., Vigevano, L., 2002. Roe linearization for the van der Waals gas. *J. Comput. Phys.* 175 (1), 50–78.
- Guardone, A., Vimercati, D., 2016. Exact solutions to non-classical steady nozzle flows of Bethe-Zel'dovich-Thompson fluids. *J. Fluid Mech.* 800, 278–306.
- Harten, A., 1983. High resolution schemes for hyperbolic conservation laws. *J. Comput. Phys.* 49 (3), 357–393.
- Harten, A., Hyman, J. M., 1983. Self adjusting grid methods for one-dimensional hyperbolic conservation laws. *J. Comput. Phys.* 50 (2), 235–269.
- Hayes, W. D., 1958. The basic theory of gasdynamic discontinuities. In: Emmons, H. W. (Ed.), *Fundamentals of gasdynamics*. Vol. 3 of *High speed aerodynamics and jet propulsion*. Princeton University Press, Princeton, N.J., pp. 416–481.
- Kermani, M., Plett, E., 2001. Modified entropy correction formula for the roe scheme. In: 39th Aerospace Sciences Meeting and Exhibit. p. 83.

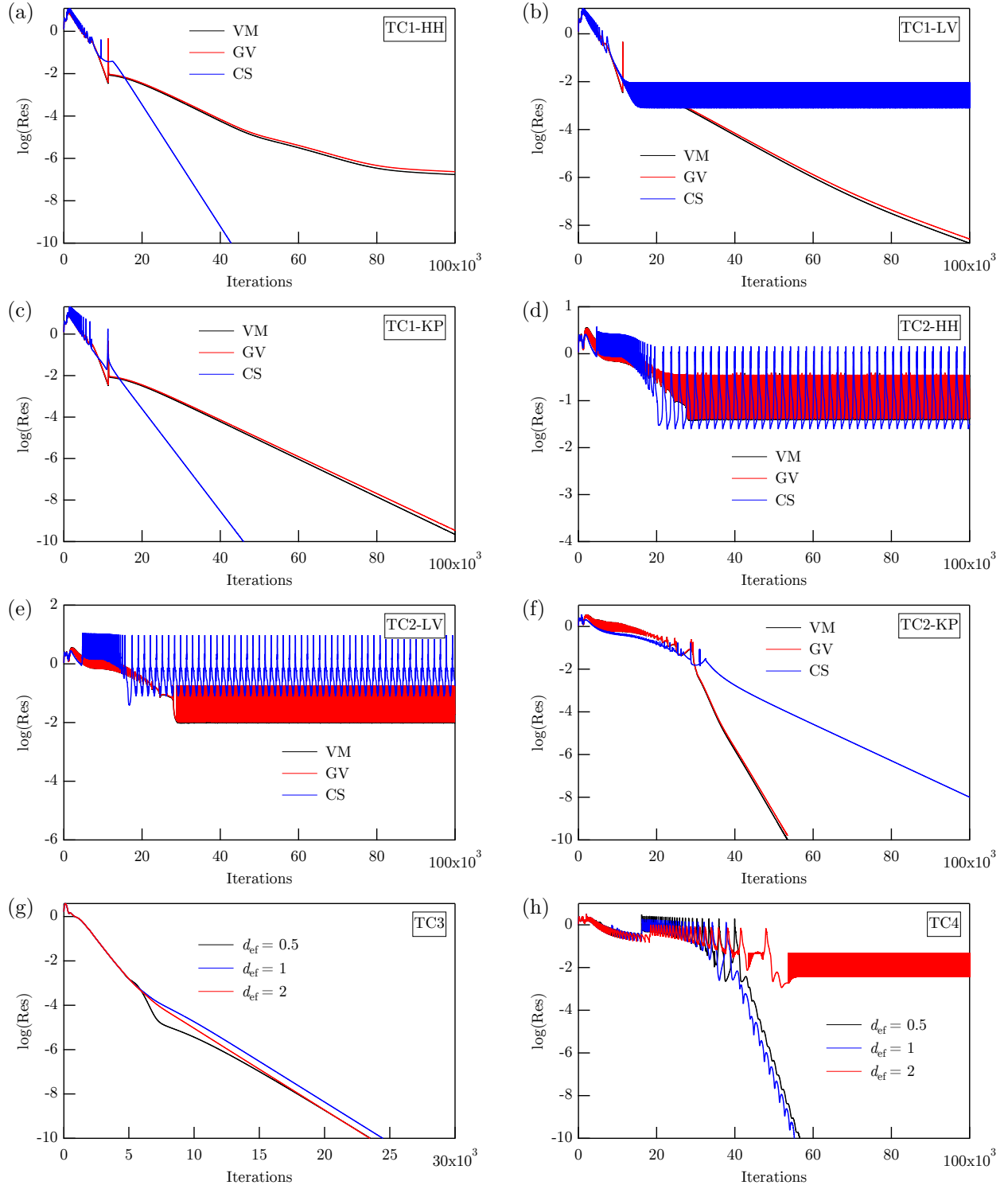


Figure 13: Convergence history for each of the test cases.

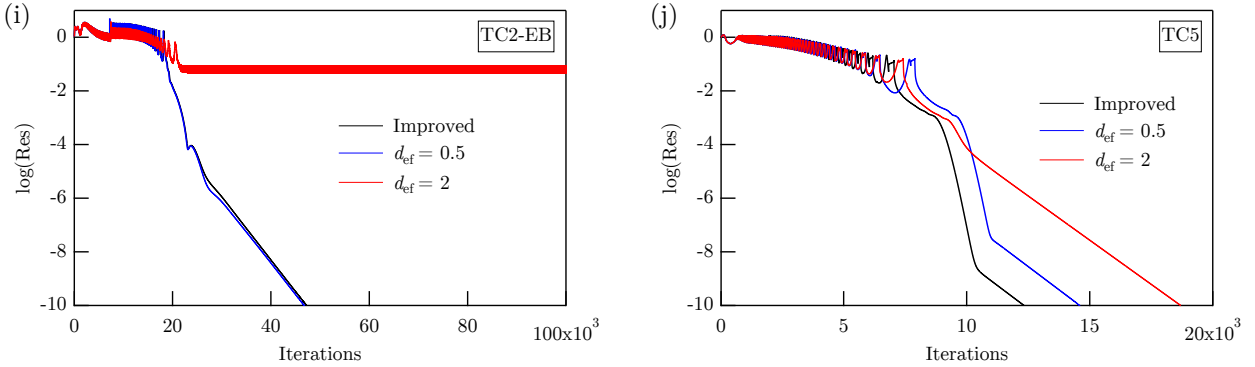


Figure 13 (Cont.): Convergence history for each of the test cases.

- Kluwick, A., 1993. Transonic nozzle flow of dense gases. *J. Fluid Mech.* 247, 661–688.
- Kluwick, A., 2004. Internal flows of dense gases. *Acta Mech.* 169, 123–143.
- LeVeque, R. J., 1992. Numerical methods for conservation laws. Vol. 132. Springer, Ch. 9, pp. 151–156.
- LeVeque, R. J., 1998. Balancing source terms and flux gradients in high-resolution Godunov methods: the quasi-steady wave-propagation algorithm. *J. Comput. Phys.* 146 (1), 346–365.
- LeVeque, R. J., 2011. A well-balanced path-integral f-wave method for hyperbolic problems with source terms. *J. Sci. Comput.* 48 (1-3), 209–226.
- Liou, M. S., Van Leer, B., Shuen, J.-S., 1990. Splitting of inviscid fluxes for real gases. *J. Comput. Phys.* 87 (1), 1–24.
- Masella, J. M., Faille, I., Gallouët, T., 1999. On an approximate Godunov scheme. *Int. J. Comput. Fluid Dyn.* 12 (2), 133–149.
- Menikoff, R., Plohr, B. J., 1989. The Riemann problem for fluid flow of real materials. *Rev. Mod. Phys.* 61(1), 75–130.
- Mottura, L., Vigevano, L., Zaccanti, M., 1997. An evaluation of Roe's scheme generalizations for equilibrium real gas flows. *J. Comput. Phys.* 138 (2), 354–399.
- Müller, S., Voß, A., 2006. The Riemann problem for the Euler equations with nonconvex and nonsmooth equation of state: construction of wave curves. *SIAM J. Sci. Comput.* 28 (2), 651–681.
- Roe, P. L., 1981. Approximate Riemann solvers, parameter vectors, and difference schemes. *J. Comput. Phys.* 43 (2), 357–372.
- Roe, P. L., 1987. Upwind differencing schemes for hyperbolic conservation laws with source terms. Springer Berlin Heidelberg, Berlin, Heidelberg, pp. 41–51.
- Thompson, P. A., 1971. A fundamental derivative in gasdynamics. *Phys. Fluids* 14 (9), 1843–1849.
- Thompson, P. A., 1988. Compressible Fluid Dynamics. McGraw-Hill.
- Thompson, P. A., Lambrakis, K. C., 1973. Negative shock waves. *J. Fluid Mech.* 60, 187–208.
- Toro, E. F., 2013. Riemann solvers and numerical methods for fluid dynamics: a practical introduction. Springer Science & Business Media.
- Toumi, I., 1992. A weak formulation of Roe's approximate Riemann solver. *J. Comput. Phys.* 102 (2), 360–373.
- van der Waals, J. D., 1873. Over de continuïteit van den gas - en vloeistofstoestand (on the continuity of the gas and liquid state). Ph.D. thesis, Leiden University.
- van Leer, B., Lee, W. T., Powell, K. G., 1989. Sonic-point capturing. AIAA paper 1945, 1989.
- Vinokur, M., Montagné, J. L., 1990. Generalized flux-vector splitting and Roe average for an equilibrium real gas. *J. Comput. Phys.* 89 (2), 276–300.
- Weyl, H., 1949. Shock waves in arbitrary fluids. *Comm. Pure Appl. Math.* 2 (2-3), 103–122.
- Zamfirescu, C., Dincer, I., 2009. Performance investigation of high-temperature heat pumps with various BZT working fluids. *Thermochim. Acta* 488 (1), 66–77.
- Zamfirescu, C., Guardone, A., Colonna, P., March 2008. Admissibility region for rarefaction shock waves in dense gases. *J. Fluid Mech.* 599, 363–381.
- Zel'dovich, Y. B., 1946. On the possibility of rarefaction shock waves. *Zh. Eksp. Teor. Fiz.* 4, 363–364.